Pulsed photothermal evaluation of layered materials

Cielo, P.

Publisher's version / Version de l'éditeur:
https://doi.org/10.1063/1.333758
Journal of Applied Physics, 56, 1, pp. 230-234, 1984-07-01

RESEARCH ARTICLE | JULY 01 1984

Pulsed photothermal evaluation of layered materials

P. Cielo

J. Appl. Phys. 56, 230–234 (1984)
https://doi.org/10.1063/1.333758

Pulsed photothermal evaluation of layered materials

P. Cielo
Industrial Materials Research Institute, National Research Council of Canada, 75 De Mortagne Boulevard, Boucherville, Quebec, Canada, J4B 6Y4

(Received 16 January 1984; accepted for publication 9 March 1984)

A pulsed photothermal technique is described for the nondestructive evaluation of stratified materials. The time history of the surface temperature after the absorption of a short laser pulse is used to obtain information about the subsurface structure and the thermophysical properties of the material. Applications to the inspection of plasma-sprayed coatings and graphite-epoxy laminates are presented.

I. INTRODUCTION

Photoacoustic and photothermal techniques have recently been applied successfully to the evaluation of thin films.[1,2] Such techniques are based on the monitoring of either the amplitude or the phase of thermal waves which are generated by a chopped laser beam incident on the film surface. A similar approach has been used for the detection of subsurface cracks.[3] Temperature probing at the heated surface can be done with a photoacoustic cell,[2,3] or through laser-beam deflection by thermal lens or thermal deformation effects,[1] or else using an IR detector.[4] The application of similar techniques to the analysis of thicker films, such as plasma-sprayed coatings or surface-hardened layers, has also been reported recently.[4–6] Thermal inspection techniques appear to be a powerful tool for materials' evaluation. It may be mentioned, as an example, that the thermal conductivity of steel changes by a factor of 2 after hardening,[4] as compared to a variation of the order of 1% in the ultrasonic velocity.[7]

In this paper, a pulsed photothermal technique for the evaluation of thick layers or laminated materials is described. The inspected surface is heated by a single laser pulse, and the thermal history curve is monitored by a focused IR detector. The pulsed approach is faster than the chopped-laser method because it requires only one thermal cycle. Time considerations may become important when thick layers of low thermal conductivity must be inspected, or when large surfaces must be scanned. Moreover, the pulsed thermal analysis is directly applicable to the real-time control of pulsed thermal treating processes.[8]

Thermally-sprayed metallurgical coatings are widely used to increase the wear and corrosion resistance of bare metallic surfaces. The possibility to inspect nondestructively such coatings, which are usually tested destructively, is of great interest for the manufacturing industry.[9] The parameters which are of interest in such coatings are their thickness, adhesive, and cohesive strength. Cohesive failure of the coating takes place when cracks develop within the coating; this is usually caused by improper spraying parameters resulting in porosity or particle-to-particle unbonds within the layer. Adhesive failure occurs when the coating detaches from the substrate under stress. Typical lack-of-adhesion defects are coating-to-substrate unbonds or delaminations usually caused by improper surface preparation of the substrate. In order to verify the effectiveness of our technique, some aluminium coatings were plasma sprayed on aluminium substrates, with or without artificial defects at the coating-substrate interface.

II. THEORETICAL MODEL

In the experiments which will be described in the next section, a CO_2-TEA laser with volumetric ratio equal to 0.05 was used to obtain 60 mJ, 50 μs pulses with a pulse shape optimized ot obtain efficient surface heating without overheating.[10] The single-transversal-mode pulse has a gaussian distribution with $1/e^2$ radius of 4 mm, which is much larger than the 200-μm thickness of the coatings. In such circumstances, we can represent in a first approximation the temperature history within a homogeneous sample, after absorption of the pulse, by the one-dimensional model for an instantaneous pulse[11,12]:

$$T(z,t)=\frac{Q}{(\pi K\rho c t)^{1/2}}\exp\left(\frac{-z^2}{4\alpha t}\right), \tag{1}$$

where z and t are, respectively, the depth and time variables, Q is the injected energy density, K is the thermal conductivity, ρ is the density, c the specific heat, and $\alpha = K/\rho c$ is the thermal diffusivity. We can see from Eq. (1) that the surface temperature ($z = 0$) of a homogeneous sample decays as $(t)^{-1/2}$ after the absorption of the pulse.

The effect of the finite pulse duration and of the sample inhomogeneity can be best analyzed by a finite difference numerical model.[13] The surface temperature history obtained from such a model is shown in Fig. 1. In this figure, curve (a) represents the thermal history after the absorption of a 50-μs pulse by a homogeneous steel sample ($K = 0.7$ W/cm °C, $\rho = 7.8$ g/cm^3, and $c = 0.5$ J/g °C). We can see that, apart from an initial perturbation caused by the finite pulse duration, the thermal decay slope is equal to $-1/2$ on the log-log scale, in agreement with Eq. (1). Curve (b) corresponds to a nickel-chrome layer ($K = 0.14$ W/cm °C), 100-μm thick, over a steel ($K = 0.7$ W/cm °C) substrate. The curve slope presents a discontinuity when the thermal front reaches the interface after a period which is of the order of the thermal propagation time $t \approx l^2/4\alpha$ through the thickness l of the coating. The position of this discontinuity can thus be used to obtain the coating thickness l if its thermal diffusivity is known. Moreover, the vertical displacement T_l

 0021-8979/84/130230-05$02.40

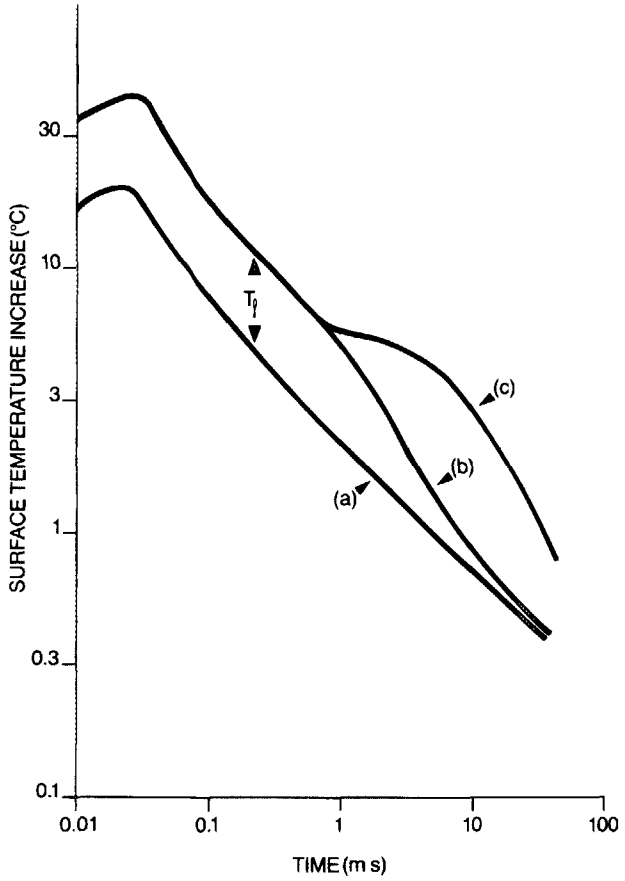

FIG. 1. Calculated thermal decay curves for a plasma-sprayed coating heated by a 50-μs pulse. Curve (a): bare steel sample; curve (b): well-bonded Ni-Cr coating on steel substrate; curve (c): delaminated coating.

between the coated-sample curve (curve b) and its asymptote for large values of t (curve a) can be used to obtain the ratio between the effusivity $e = K\rho c$ of the coating and the substrate:

$$T_l = \frac{1}{2} \log \frac{e_s}{e_c}, \tag{2}$$

as can be inferred from Eq. (1). This is an interesting possibility because the thermal parameters of the substrate are usually well known, while the properties of the coating depend on the spraying process parameters. Curve (c) corresponds to an unbonded coating where the interface defect has been represented by a 1-μm-thick air layer.[14] The presence of the defect is apparent in this curve.

The surface temperature variation is monitored by an IR detector focused in the center of the heated area. The amplitude of the detector signal as a function of the temperature can be written[15]:

$$V = CT^n, \tag{3}$$

where n approaches the value:

$$n = 5\frac{\lambda_m}{\lambda} \quad \text{for} \quad \frac{\lambda}{\lambda_m} < 2.5, \tag{4}$$

λ is the center wavelength of the detector bandwidth, λ_m is the peak emission wavelength of the Planck spectral radiation curve at the operating temperature, and T is the temperature in degrees Kelvin. In our experiments, we had $\lambda \approx 5$ μm and $\lambda_m \approx 10\,\mu$m, so that $n \simeq 10$ in such a case. The constant C in Eq. (3) depends on the temperature-dependent emissivity of the surface, the angular aperture and voltage sensitivity of the detector, as well as the angle of observation in the case of smooth metallic surfaces.[16] As such parameters are difficult to predict in a theoretical model, the conversion from the detected signal to the temperature history curve may present some difficulty. However, most often the maximum temperature elevation $T - T_0$ is much smaller than the initial temperature T_0, which is usually of the order of 300 degrees Kelvin, so that the ac component of the signal can be written from Eq. (3):

$$V - V_0 \simeq nCT_0^{n-1}(T - T_0), \tag{5}$$

showing that the detected signal is proportional to the temperature variation if $T - T_0 \ll T_0$.

III. EXPERIMENTAL RESULTS

Figure 2 shows the experimental curves obtained from a sample without (curve a) and with (curve b) defect at the coating-substrate interface. The curves were obtained by monitoring the temperature in the center of the 8-mm-diam pulsed-laser irradiated surface with a focused InSb IR detector. The detector was previously calibrated using a thermocouple in contact with the slowly heated sample. The sam-

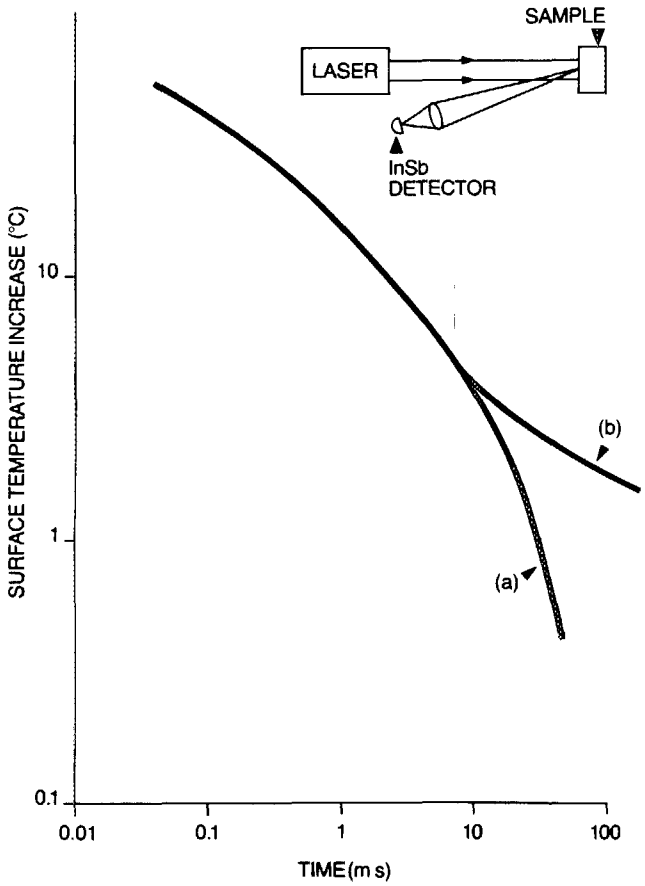

FIG. 2. Experimental curves obtained with an aluminum-sprayed aluminum sample. Curve (a): sample without defect; curve (b): sample with artificial defect at the coating-substrate interface. The insert shows the experimental configuration.

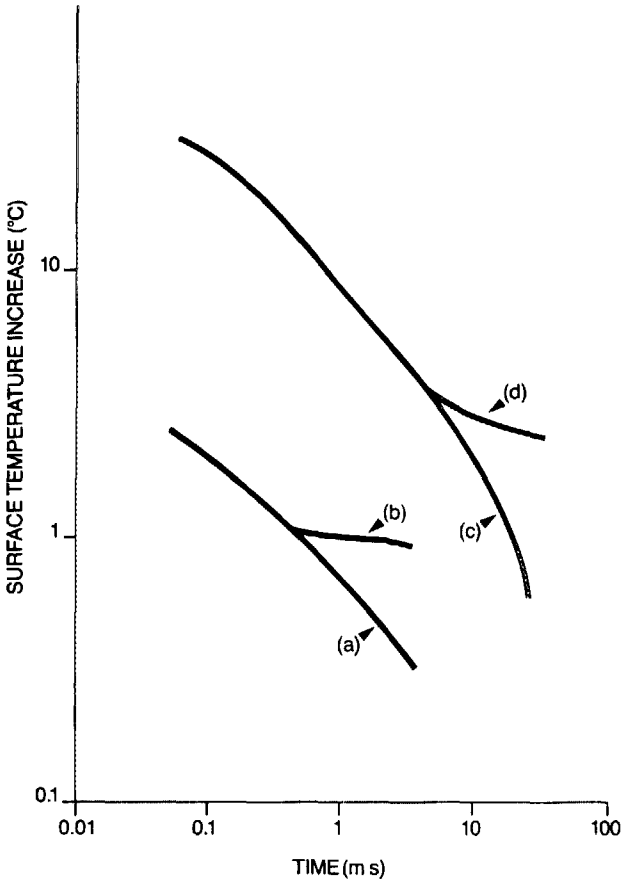

FIG. 3. Theoretical model used to interpret the experimental curves of Fig. 2. Curves (a) and (b): calculated curves for a sample without and with defect, respectively, for an Al-coating having the same thermal conductivity as the substrate; curves (c) and (d): sample without and with defect, respectively, for a thermal conductivity of the coating equal to 1/20 of the thermal conductivity of the substrate.

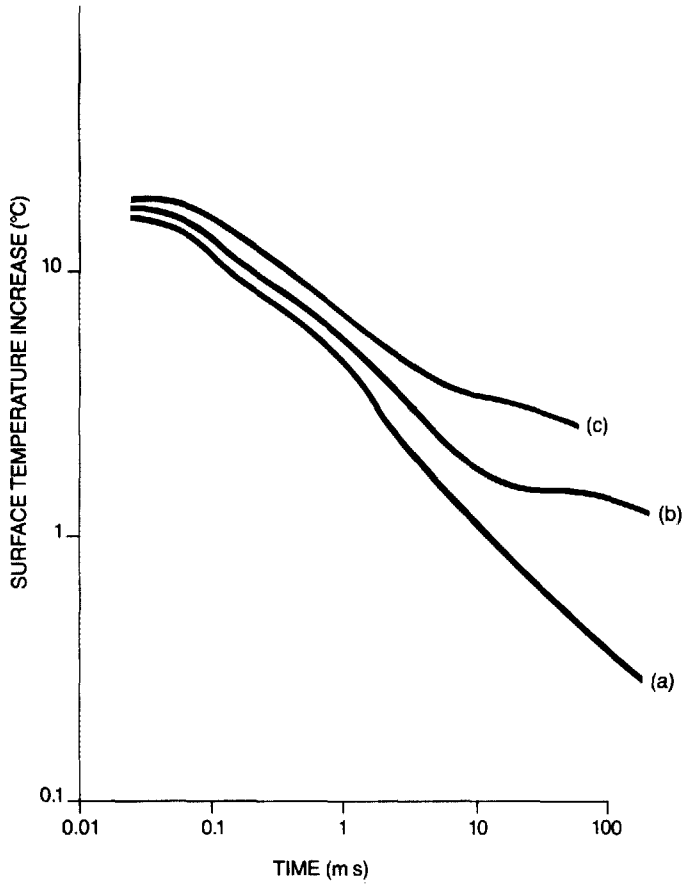

FIG. 4. Experimental curves obtained with a graphite-epoxy laminated sheet. (a): Well-bonded area; (b) and (c): delaminated regions.

ples were aluminium substrates with 200-μm-thick anodyzed aluminium coatings plasma sprayed in air. An interface defect was produced by placing a 50-μm-thick Teflon foil on the substrate before spraying the coating. The thermal conductivity of such a layer is equivalent to that of a 2-μm-thick air layer. The presence of the interface defect is clearly seen from the experimental curves of Fig. 2.

In order to interpret the experimental curves of Fig. 2, a three-dimensional, axially symmetric numerical model taking into account the gaussian-shaped laser intensity distribution and the finite spot size of the focused IR detector was used. The results are given in Fig. 3. It was first assumed that the aluminium coating had thermal properties similar to those of the aluminium substrate. Curves (a) and (b) were obtained in this case for a sample without and with defect, respectively. Both the shape of such curves and the thermal propagation time to the coating-substrate interface (0.5 ms, rather than 10 ms for Fig. 2) are significantly different from the experimental curves shown in Fig. 2. Curves (c) and (d) of Fig. 3, which are in satisfactory agreement with the experimental results, were obtained by assuming a thermal conductivity of 0.1 W/cm °C for the coating and of 2.1 W/cm °C for the substrate, the latter value corresponding to the conductivity of bulk aluminium. This suggests that the thermal properties of the coating material are strongly affected by the thermal spraying or by the anodyzation process. The *in situ* thermal analysis of thermally-sprayed coatings may thus provide a powerful tool for the evaluation of coating properties such as porosity or particle-to-particle diffusion bonding, which are related to the cohesive strength of the coating layer.

The same technique was used to analyze a graphite-epoxy laminated material which is widely used in the aircraft industry. The inspected sheet consists of four (4) layers of Hercules AS 3501-6 prepreg bonded together with equal orientation. Each layer has a thickness of 125 μm and is composed of a large number of equally-oriented, 8-μm-diam graphite fibers embedded in an epoxy matrix. The experimental results obtained with such a material are shown in Fig. 4. Curve (a) corresponds to a well-bonded region, while curves (b) and (c) were obtained on regions where the upper layer was partially unbonded. The discontinuity in the slope of curves (b) and (c) after approximately 10 ms corresponds to the expected thermal properties of the graphite-epoxy unbonded layer.

IV. DISCUSSION

While the slope of curve (a) is nearly equal to $-1/2$, as for a uniform sample, curve (c) has a significantly different slope, even before 10 ms. This may be interpreted by taking into account the heterogeneous nature of this material. Fig-

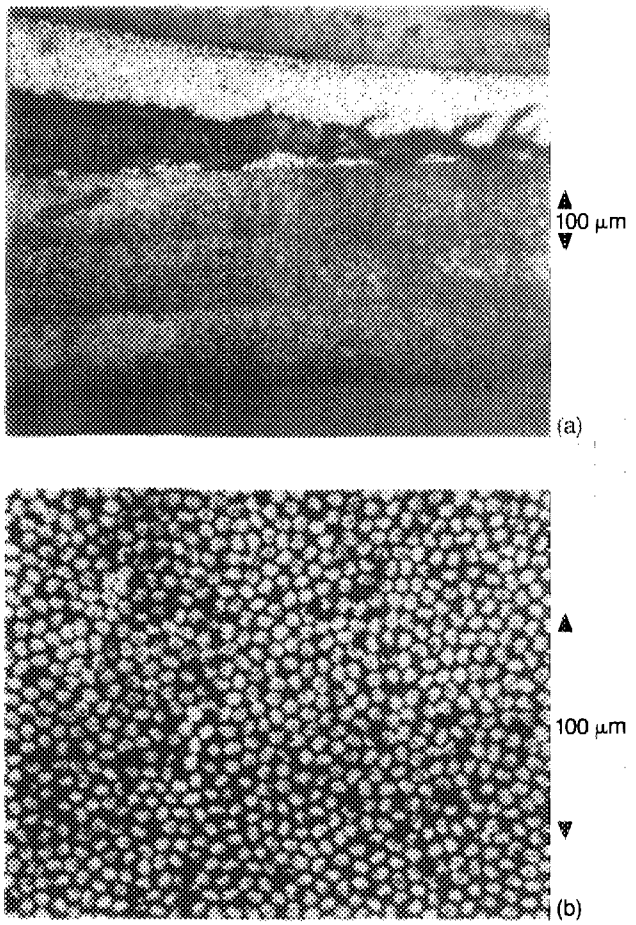

FIG. 5. (a): Cross section of the four-ply graphite-epoxy laminate used in the experiments whose results are shown in Fig. 4; (b): close-up view of the fiber-epoxy matrix.

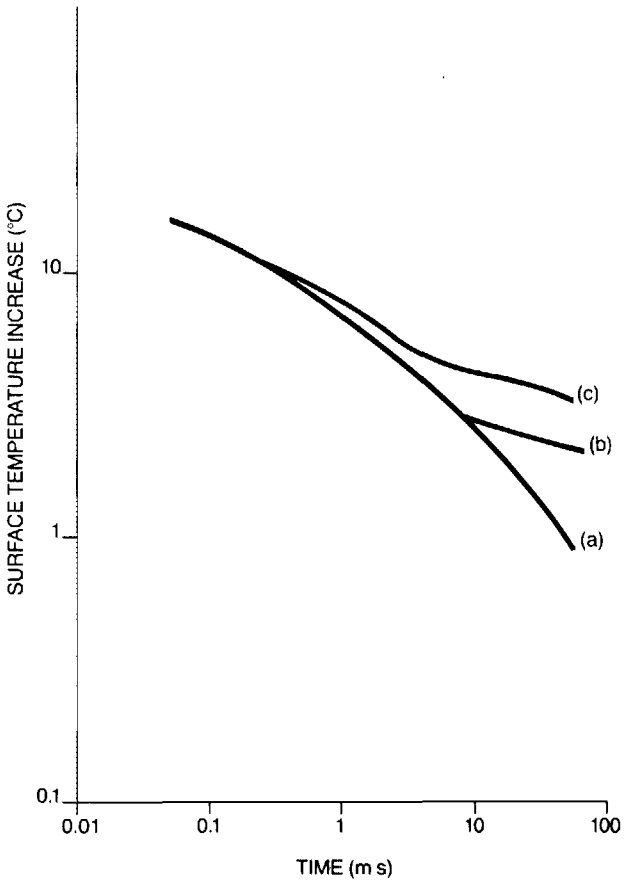

FIG. 6. Theoretical curves obtained for a graphite-epoxy laminated sample. Curve (a): well-bonded sample; curve (b): delaminated layer, uniform fiber distribution; curve (c): delaminated layer, random fiber distribution.

ure 5(a) shows a micrograph of the polished cross section of the four-ply sheet, while Fig. 5(b) shows a close-up view of the fibers. As can be seen, the fibers are randomly distributed in the matrix, some fibers being in contact with each other while other fibers are separated by a significant thickness of resin. As the thermal conductivity of epoxy, 4×10^{-3} W/cm °C is much smaller than the conductivity of graphite fibers,[17,18] 0.5 W/cm °C, the fiber distribution may significantly affect the transverse thermal properties of the composite.

Figure 6 shows the results of the fiber distribution in the composite matrix. In the three-dimensional model, 25 μm$\times$25 μm$\times$1 cm graphite elements are embedded in an epoxy matrix with volume ratio of 0.5. A contact thermal resistance equivalent to 2.5 μm of epoxy is assumed between adjacent graphite elements. Curves (a) and (b) in Fig. 6 correspond to a well-bonded and delaminated layer, respectively, with a uniformly distributed graphite-epoxy mesh, as shown in Fig. 7(a). Curve (c) in Fig. 6 corresponds to a delaminated layer with a random matrix obtained by a random-number generator, Fig. 7(b). We can see that curve (c) has a more gradual slope, similar to the experimental curve (c) of Fig. 4. These results suggest that photothermal techniques may

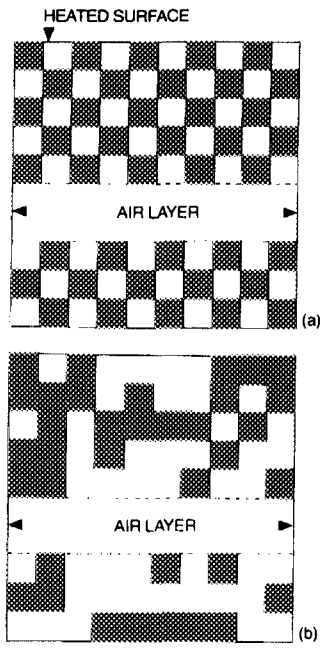

FIG. 7. Cross section of part of the fiber matrix used for the numerical models of Fig. 6. (a): Uniform matrix; (b): randomly distributed fiber matrix.

provide information not only on the presence of subsurface delaminations, but also on the fiber content and distribution in fiber-resin composite materials.

V. CONCLUSION

In conclusion, a pulsed photothermal technique has been applied to the inspection of coated and laminated industrial materials, and the results are quite encouraging. This technique is attractive because it is noncontact, easy to scan over a large surface, while it requirs no photoacoustic cell nor complex interferometric or laser-deviation devices. As the slope of the thermal history signal is observed, rather than its absolute level, this technique can be used even if the emissivity changes over the surface. Although the sensitivity of this technique is lower than that of chopped-beam techniques with long integration time, the pulsed inspection is faster and the results easier to interpret. Moreover, the pulsed approach permits to improve the signal/noise ratio by time-averaging the signal for a longer period (because of the logarithmic scale in the thermal-decay curves) in the last portion of the curve, when averaging is mostly needed because of the low level of the signal.

ACKNOWLEDGMENTS

The author wishes to thank M. Verrault and F. Beaumont of Gen-Tec Inc. for their technical support in using their laser as well as S. Dallaire of IMRI and E. P. Parkinson of Canadair Inc. for supplying the plasma-coated and the graphite samples.

Note added in proof: The author has recently become aware that similar work on pulsed photothermal inspection of thin films is being pursued by another research group.[19] Although the signal processing techniques and the type of materials inspected are different, the basic principle is similar to the one reported here.

[1] A. Rosencwaig, J. Opsal, and D. L. Willenborg, Appl. Phys. Lett. **43**, 166 (1983).
[2] R. T. Swimm, Appl. Phys. Lett. **42**, 955 (1983).
[3] K. R. Grice, L. J. Inglehart, L. D. Favro, P. K. Kuo, and R. L. Thomas, J. Appl. Phys. **54**, 6245 (1983).
[4] J. Jaarinen and M. Luukkala, Proc. 3rd Int. Top. Meeting on Photoacoustic and Photothermal Spectroscopy, Paris, April 5–8, 1983.
[5] D. P. Almond, P. M. Patel, and H. Reiter, Proc. 3rd Int. Top. Meeting on Photoacoustic and Photothermal Spectroscopy, Paris, April 5–8, 1983.
[6] S. Aithal, G. Rousset, L. Bertrand, P. Cielo, and S. Dallaire, Int. Conf. on Metallurg, Coatings, San Diego, April 9–13, 1984.
[7] C. Flambard and A. Lambert, Mec. Mater. Electr. **317**, 25 (1976).
[8] S. Dallaire and P. Cielo, Thin Solid Films **108**, 19 (1983).
[9] H. D. Steffens and H. A. Crostack, Thin Solid Films **83**, 325 (1981).
[10] S. Dallaire and P. Cielo, Metall. Trans. B **13**, 479 (1982).
[11] H. S. Carslaw and T. C. Jaeger, *Conduction of Heat in Solids* (Oxford University, Oxford, 1959), Chap. 10.
[12] J. F. Ready, *Effects of High-Power Laser Radiation* (Academic, New York, 1971).
[13] P. Cielo, 14th Symp. on Non-Destructive Evaluation, San Antonio, April 19–21, 1983.
[14] H. H. Chaskelis and A. V. Clark, Mater. Eval. **38**, 20 (1980).
[15] W. D. Lawson and J. W. Sabey, in *Research Techniques in NDT*, edited by R. S. Sharpe (Academic, London, 1970), Chap. 4.
[16] E. M. Sparrow and R. D. Cess, *Radiation Heat Transfer* (McGraw-Hill, New York, 1978), Sec. 2-2.
[17] W. Fritz, W. Hüttner, K. Maier, and R. Brandt, Rev. Int. Hautes Temp. Refract. **16**, 350 (1979).
[18] D. L. Balageas and A. M. Luc, 18th AIAA Thermophysics Conference, Montreal, June 1–3, 1983.
[19] W. P. Leung and A. C. Tam, Opt. Lett. **9**, 93 (1984).